Compositional and size-dependent spectroscopic shifts in charged self-assembled $In_xGa_{1-x}As/GaAs$ quantum dots

Gabriel Bester and Alex Zunger
National Renewable Energy Laboratory, Golden, Colorado 80401, USA
(Received 23 May 2003; published 29 August 2003)

Atomistic pseudopotential many-body calculations of excitonic (X) recombination in charged, self-assembled $In_xGa_{1-x}As/GaAs$ dots predict and explain remarkable trends. (i) The redshift of the exciton energy upon negative charging is rapidly reduced with increasing the In content and increasing the dot height. The opposite behavior is observed upon positive charging. (ii) The recombination peak energies of different charge states show intriguing symmetries and alignments, e.g., X^- aligns with X^{2-} and X^{3-} aligns with X^{4-}. (iii) The X^{3-} spectrum shows that a triplet initial state is lower in energy for flat dots (yielding two spectral lines), whereas the singlet state is lower in energy for taller dots (yielding a single line). These trends are explained theoretically in terms of a crossover occurring at a critical In concentration and dot height at which the electron wave functions becomes more localized than the hole wave functions.

DOI: 10.1103/PhysRevB.68.073309 PACS number(s): 73.21.La, 71.35.Pq, 78.67.Hc, 71.10.−w

While early optical measurements on self-assembled quantum dots were performed on neutral dots, device applications of these structures often involve the presence of charge. This is the case when transport is involved[1,2] or in the context of quantum computation where the trion state (two electrons and one hole) is proposed to play a central role[3,4]. Recent advances in single-dot spectroscopy made it possible to selectively charge a dot by a certain number of electrons or holes and study the effects of the presence of these additional, ''spectator'' charges on the excitonic photoluminescence (PL) spectra.[5–16] Intriguing features were revealed, for instance, the fundamental excitonic PL line shifts to the red (blue) as the dot is charged by additional electrons (holes), new lines appear for dot charges $Q=\pm 2$ and for $Q=\pm 4$ and PL peaks of different charge states (e.g., X^{2-} and X^-) tend to surprisingly align. Whereas all of these effects were seen experimentally in $In_xGa_{1-x}As/GaAs$ dots, except in special cases[17,18] the geometry and composition of these dots are generally unknown. It is thus important to establish theoretically the link between dot geometry/composition and the intriguing charging effects. In this paper we therefore provide quantitative predictions on the effects of composition dependence and of confinement (size dependence) on the charging spectra of $In_xGa_{1-x}As/GaAs$ dots and explain the underlying physics in the calculated trends. We find that (a) the redshift of the exciton energy upon negative charging is reduced rapidly as the In content of the dot x increases and as the dot height h increases and (b) the charged spectrum of certain alloyed dots exhibits a striking alignment of peaks which is in agreement with recent experimental observations. We analyze our numerical results in terms of a simple stepwise model and isolate the effects of (i) the direct Coulomb interaction, (ii) the exchange Coulomb interaction, and (iii) the effect of correlations. We show that both effects, (a) and (b) reflect the existence of a surprising crossover between the electron versus hole localization at a certain composition and dot height.

A predictive calculation of spectra of charged exciton is a challenge. It is not accessible to effective mass theory for two reasons. First, this method uses as starting assumption an artificially higher symmetry[19] which yields spurious degeneracies (e.g., the P state in cylindrical dots). Second, it assumes a given confining potential or level spacing at the outset[7,20–22] and therefore does not provide a link between dot composition and the resulting excitonic spectra.

Here we use the empirical plane-wave pseudopotential method[23] to describe the single-particle problem, and the configuration interaction (CI) method[24] to describe many-body correlation effects. The total pseudopotential $V(\boldsymbol{r})=\Sigma_{\alpha,n}v_\alpha(\boldsymbol{r}-\boldsymbol{R}_n)$ is given as a superposition of screened atomic pseudopotentials v_α (with $\alpha=$Ga, In, As) centered around each atom at $\boldsymbol{R}_n$. The atomistic character naturally includes the effect of strain, alloy fluctuations, composition gradients, and spin-orbit interactions. Most important in the results that follow are the electrostatic interactions between the particles, given by the two center Coulomb integrals

$$\langle \psi_i^a \psi_j^b|\hat{U}|\psi_{j'}^b,\psi_{i'}^a\rangle=\int\int \frac{\psi_i^\star(\boldsymbol{r}_a)\psi_j^\star(\boldsymbol{r}_b)\psi_{j'}(\boldsymbol{r}_b)\psi_{i'}(\boldsymbol{r}_a)}{\epsilon(\boldsymbol{r}_a,\boldsymbol{r}_b)|\boldsymbol{r}_a-\boldsymbol{r}_b|}d\boldsymbol{r}_a d\boldsymbol{r}_b \tag{1}$$

where the dielectric function ϵ is calculated using the model of Resta.[25] These integrals can be classified into three different categories: (1) the direct Coulomb integrals $\langle \psi_i^a\psi_j^b|\hat{U}|\psi_j^b\psi_i^a\rangle\equiv J_{ij}$, (2) the exchange Coulomb integrals $\langle \psi_i^a\psi_j^b|\hat{U}|\psi_i^b\psi_j^a\rangle\equiv K_{ij}$, and (3) the scattering integrals $\langle \psi_i^a\psi_j^b|\hat{U}|\psi_{j'}^b,\psi_{i'}^a\rangle$ with $i\neq i'$ and $j\neq j'$. The CI expansion includes Slater determinants made of twelve electron and twelve hole states. The method and the pseudopotentials v_α have been used successfully previously, for instance, in Refs. 26,27.

Results of the full CI calculation. The calculated excitonic spectra for different charged states Q, labeled as X^Q, are shown as the solid peaks in Fig. 1. We consider here a lens-shaped $In_xGa_{1-x}As$ dot [base $(b)=20$ nm, height $(h)=5$ nm] with an onionlike composition profile with x reaching from 0.8 in the core to 0.2 at the outer boundary of the dot. This choice for this size and composition profile is inspired from the experiments of Walther *et al.*[17] and Kegel *et al.*[18] All calculated dots are embedded in GaAs and have

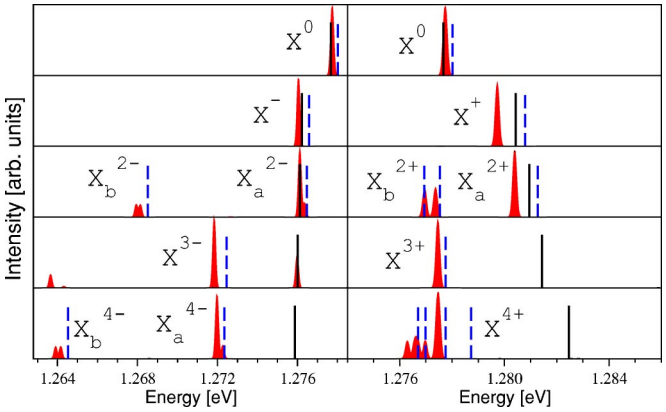

FIG. 1. (Color online) Calculated PL spectra for different charged states of the onion (see text) InGaAs lens-shaped ($b=20$ nm, $h=5$ nm) dot. The solid peaks are the results of the full CI calculations. The dashed (solid) lines are obtained neglecting correlation (correlation and exchange) effects.

one monolayer thick InGaAs wetting layer. Figure 2 shows the relative shifts of the main X^0, $X^{-/+}$, and $X^{2-/2+}$ peaks (as defined in the caption) as a function of the In composition x and the height of the dot h. The main features of the calculated spectra are as follows.

(i) The shifts A^+ vs A^- as well as B^+ vs B^- show opposite trends as function of the composition and height: A^+ and B^+ increase with increasing In composition and height, while A^- and B^- decrease with x and h. There is a crossover of (A^+, A^-) and (B^+, B^-) at $\approx$80% In and at $\approx$4.6 nm dot height.

(ii) The excitonic structure of the negatively charged onion dot in Fig. 1 presents some striking peak symmetries and alignments: The X^- and X_a^{2-} transitions are aligned; the main peak of X^{3-} is located midway between the X_a^{2-} and the X_b^{2-} transitions and is aligned with the X_a^{4-} peak.

(iii) Three transitions are observed in the X^{3-} spectrum in Fig. 1, in contradiction with previous models which start from degenerate electron P states and predict two peaks.[15,20,21,28–30] In Ref. 8 the authors expect either two or one peak depending on the splitting of the electron P states.[8]

Comparison with experiment. We selected two dots that

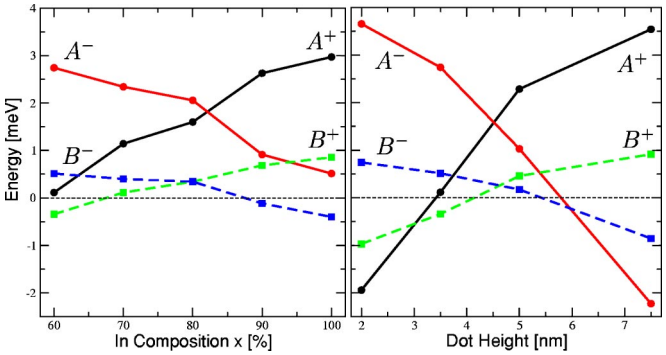

FIG. 2. (Color online) Spectroscopic shifts $A^+=X^0-X^+$, $A^-=X^0-X^-$ (both solid lines), $B^+=X^+-X_a^{2+}$, $B^-=X^--X_a^{2-}$ (both dashed lines) as a function of composition (for a lens-shaped dot of base 25 nm and height 3.5 nm) and height (for an $In_{0.6}Ga_{0.4}As$ lens-shaped dot with 25 nm base).

TABLE I. Compilation of the available experimental results on the spectroscopic shift in $In_xGa_{1-x}As/GaAs$ quantum dots.

	A^-	A^+	B^-	C^-
Exp. (Refs. 6–12)	3.1–5.8	−0.8−−1.5	0.0–0.5	4.1–4.9
Calc. onion	1.7	−2.0	0.2	8.1
Calc. $In_{0.6}Ga_{0.4}As$ $h=2$ nm, $b=25$ nm	3.7	−1.9	0.7	7.7

have a composition and shape close to the one suggested by some experiments:[8,17,18] the onion dot and a lens shaped $In_{0.6}Ga_{0.4}As$ dot ($b=2$ nm, $h=25$ nm). The results are compared with experiment in Table I. The measured redshift A^- (Refs. 6–16) and the blueshift A^+ (Refs. 6,13) agree very well with our calculation. Also the calculated alignment of the X^- and X_a^{2-} transitions (small values of B^-) is in excellent agreement with Refs. 8–11,13,14 and the fact that the X^{3-} transition is located midway between the X_a^{2-} and X_b^{2-} transitions is also observed experimentally in Refs. 8,13. The exchange splitting C^- on the other hand tends to be overestimated by the theory. This might be attributed to shape anisotropy effects. The calculated excitonic dipole moment for the onion dot (7.2×10^{-29}Cm) agrees well with the measured dipole of Fry *et al.*[31] $(7\pm2)\times10^{-29}$ C m and Findeis *et al.*[9] $(8)\times10^{-29}$ C m, where in all cases the holes are above the electrons.

Analysis of calculated results. In order to understand our numerical results, we present a step-by-step analysis. Figure 3 gives the energies of the different transitions, neglecting correlations, in terms of the diagonal direct Coulomb energies $J_{e_ie_j}$, $J_{e_ih_j}$, $J_{h_ih_j}$, the exchange energy between like-carriers $K_{e_ie_j}$, $K_{h_ih_j}$ [see Eq. (1)]. When the final configurations are open shell, the exchange terms will split the main transition. For example the e_0-h_0 recombination of X^{2-} results in a singlet and triplet with like-particle exchange energies 0 and $2K_{e_0e_1}$, respectively. The boxed entries in Fig. 3 interpret the energy shifts and splittings in terms of the

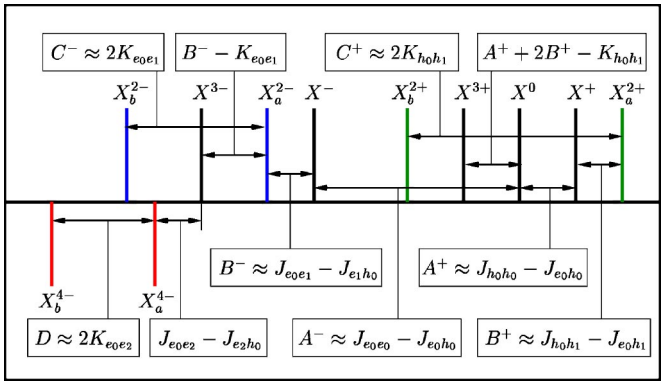

FIG. 3. (Color online) Schematic of the different excitonic shifts observed in Fig. 1. The energy shifts are given in terms of the direct Coulomb ($J_{e_ie_j}$, $J_{e_ih_j}$, and $J_{e_ie_j}$) and of the like-particle exchange ($K_{e_ie_j}$ and $K_{h_ih_j}$) terms. The electron-hole exchange terms and correlation effects are omitted for simplicity (included in Figs. 1 and 2).

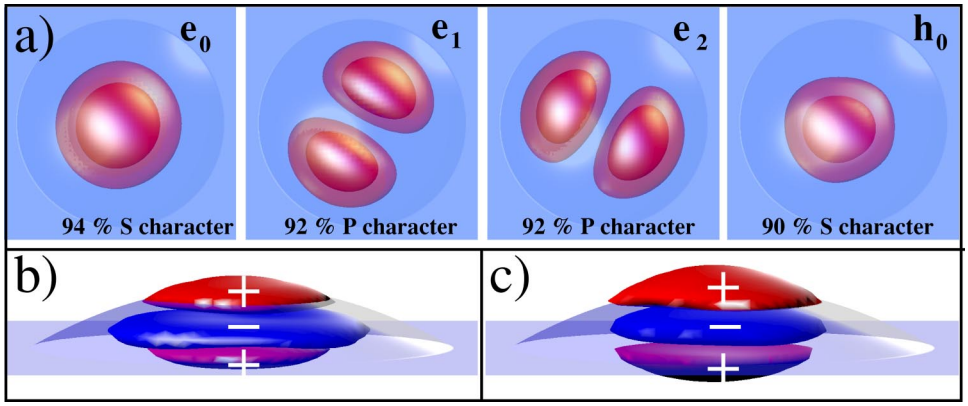

FIG. 4. (Color online) Upper panel (a) Isosurfaces enclosing 75 and 40 % of the state densities of the first three electron and the first hole states for an $In_{0.6}Ga_{0.4}As$ dot. Lower panels: Isosurfaces of the state density differences $\rho_{\mathrm{diff}}=\rho_e-\rho_h$ for a pure InAs dot (b) and for an $In_{0.6}Ga_{0.4}As$ dot (c). The electrons, compared to the holes, are more localized toward the top and base of the dots. All dots are lens shaped ($b=25$ nm, $h=3.5$ nm).

Coulomb and like-particle exchange terms, neglecting the very small electron-hole exchange terms $K_{e_ih_j}$ (included in Figs. 1 and 2). We can now interpret the main splittings in terms of specific interactions: The two main peaks for $Q=$even reflect like-carrier exchange interactions: the $X_a^{2-}-X_b^{2-}=C^-$ splitting is $2K_{e_0e_1}$, whereas the $X_a^{4-}-X_b^{4-}=D$ splitting is $2K_{e_0e_2}$. On the other hand, the $0\rightarrow(\pm1)\rightarrow(\pm2)$ shifts reflect direct Coulomb energy differences. The $X^0-X^-=A^-$ shift is $J_{e_0e_0}-J_{e_0h_0}$, the $X^0-X^+=A^+$ shift is $J_{h_0h_0}-J_{e_0h_0}$, and the $X^--X_a^{2-}=B^-$ shift is $J_{e_0e_1}-J_{e_1h_0}$. Thus, whereas the splitting of the $Q=$even peaks reflect absolute exchange energies, the shifts A^-, A^+, B^+, B^- reflect relative Coulomb energies that vanish at zero order. Indeed, if the hole and electron wave functions were the same (as is assumed in single-band effective mass models with infinite wells), then $A^-=A^+=B^+=B^-=0$.

While Fig. 3 neglects the effect of correlations, these are taken into account in Figs. 1 and 2. To understand the effect of correlations we compare in Fig. 1 the full CI results (black peaks) with the spectra calculated without correlations (dashed lines). The effect of the exchange and scattering terms can be seen by comparing the dashed and the solid black lines (neglecting correlations and exchange integrals). Whereas the direct Coulomb energies merely shifts the PL peaks, the exchange interaction splits (X^{even}) and shifts ($X^{\pm3}$, $X^{\pm4}$) peaks. Correlation effects tend to shift peaks to the red by as much as 2 meV in the present dots. In fact, neglecting the effect of correlations would result in a downward shift by about 2 meV of the A^+ and A^- curves in Fig. 2 and leading to the wrong conclusion that In rich dots exhibit a blueshift (redshift) of the X^- (X^+), since A^- and A^+ would be negative. The B^+ and B^- curves are nearly unaffected by correlations.

Our foregoing analysis of the origins of the spectra allows us to comment on the spectroscopic observations (i)–(iii) made above.

(i) *Trends in* $X^0\rightarrow X^-$ *and* $X^0\rightarrow X^+$. We saw that the shifts A^+ and A^- in Fig. 3 reflect the balance between like-particle (e_0-e_0 or h_0-h_0) and different-particle (e_0-h_0) Coulomb interactions. In the lower panels of Fig. 4 the difference between the electron e_0 and hole h_0 densities ρ_{diff} is plotted for a pure InAs and for an $In_{60}Ga_{40}As$ dot. It shows, for both dots, that h_0 is more *localized* in the growth direction than e_0 since ρ_{diff} has a negative value (characteristic for h_0) in the center of the dot. However, in the pure InAs dot [panel (b)] h_0 is more *delocalized* in the (001) plane than e_0. In contrast, for the $In_{0.6}Ga_{0.4}As$ dot, e_0 and h_0 have equivalent localization in this plane. This effect can be appreciated by the percentage of the charge density inside the physical dimension of the dot. This yields 90.1% (88.4%) for the first hole state and 82.4% (82.8%) for the first electron state in the pure (onion) dot. For the onion dot, the stronger hole localization contributes to a negative value for A^- (since $J_{e_0h_0}$ is larger than $J_{e_0e_0}$) and a positive value for A^+ (since $J_{h_0h_0}$ is larger than $J_{e_0h_0}$). The physics underlying the observed trends is therefore related to the degree of localization of the wave functions and can be understood as follows. (1) The reduction of size (reducing the width of the potential well) increases the confinement energy of both electrons and holes, i.e., their single particle levels move up and down, respectively. Thereby, their wave functions become more delocalized. This effect is more pronounced for the electron than for the hole state: The electrons tend to be more delocalized than the holes when the size is reduced. (2) The reduction of the In content lowers the band offsets between the material in the dot and the surrounding GaAs. This reduction delocalizes electrons more strongly than holes: The electrons tend to be more delocalized than the holes when the In concentration is reduced.

(ii) *Alignment of peaks in different charged states.* The alignments evident in the spectrum of the negatively charged dot (Fig. 1) can be understood from the different integral contributions shown in Fig. 3: The X^-, X_a^{2-}, X^{3-}, and X_a^{4-} peaks are predicted to be shifted from the fundamental X^0 transition by A^-, (A^-+B^-), $(A^-+2B^--K_{e_0e_1})$, and $(A^-+2B^--K_{e_0e_1}+J_{e_0e_2}-J_{e_2h_0})$, respectively. For certain heights and compositions, $B^-=J_{e_0e_1}-J_{e_1h_0}$ is close to zero which results in the alignment of the of X_a^{2-} and X^- peaks. For B^- to vanish, the states e_0 and h_0 do not necessarily need to be identical. Unlike the shifts A^+ and A^- that involved integrals over *S*-like states only (e_0 and h_0), B^- involves a *P*-like state (e_1). In Fig. 4 the e_0, e_1 and h_0 charge densities are depicted. The overlap between e_1 and e_0 or h_0 is not a linear function of the localization anymore. Both, an extremely localized or an extremely delocalized

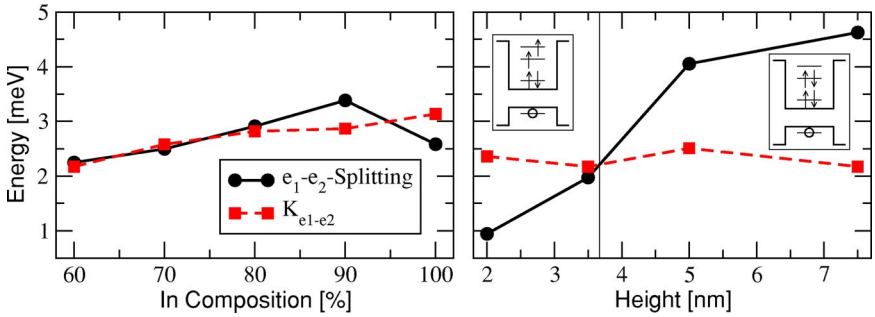

FIG. 5. (Color online) Electron-electron exchange $K_{e_1e_2}$ and energy splitting between the second and third electron states e_1 and e_2 as a function of composition (for a lens-shaped dot of base 25 nm and height 3.5 nm) and height (for an $In_{0.6}Ga_{0.4}As$ lens-shaped dot with 25 nm base).

state e_0 or h_0 would have no overlap with e_1. Our calculations show, that at a certain composition (80%) and height (4.7 nm) the contributions from $J_{e_0e_1}$ and $J_{e_1h_0}$ nearly cancel. For a very small value of B^-, the X^{3-} peak lies midway between the X_a^{2-} and X_b^{2-} peaks since it is located $K_{e_0e_1}$ away from each. The X^{3-} peak is aligned with the X_a^{4-} because $J_{e_0e_2}-J_{e_2h_0}$ nearly cancel. The reason for this cancellation is the same as the one given for the cancellation of B^- since e_1 and e_2 are very similar (see Fig. 4). We thus predict the observation of the alignments of the X^{3-} peak with the X_a^{4-} peak whenever the alignment of the X_a^{2-} and X^- peaks is observed.

(iii) *Two additional lines in* X^{3-}. For the initial state of the X^{3-} transition, two configurations are possible: the ''Aufbau'' singlet $h_0^1e_0^2e_1^2$ (right inset of Fig. 5) or the ''Hund'' triplet $h_0^1e_0^2e_1^1e_2^1$ (left inset). The excitonic decay of the singlet configuration has one channel while the triplet configuration has two channels ($e_0^{\uparrow}e_1^{\uparrow}e_2^{\uparrow}$ or $e_0^{\downarrow}e_1^{\uparrow}e_2^{\uparrow}$). Consequently in the PL spectrum one would observe either a single line or two lines. Whether the singlet or triplet configuration is preferred depends on the energy splitting between the P levels (e_1 and e_2) and on the magnitude of the exchange interaction $K_{e_1e_2}$. Both quantities are plotted as function of composition and size in Fig. 5 and are found to exhibit a crossover as a function of height: tall dots preferring the singlet configuration. The ground state of the onion dot (and of all dots where both quantities are energetically similar) is in fact, a correlated state composed of a dominant singlet component (responsible for the stronger peak in the middle of panel X^{3-} in Fig. 1) and a weaker triplet state component (responsible for the two satellite peaks). All three transitions are therefore observed.

In summary, we have shown that the physics underlying the spectra of charged quantum dots is very rich. The trends observed in the shifts A^+ and A^- are shown to be related to the crossover in the localization of electron and hole wave functions and correlation effects are shown to qualitatively change the conclusions. Quantitative predictions along with a qualitative understanding of the experimentally observed alignment of certain peaks is given. A detailed balance between exchange interaction and single particle energy is shown to be reflected in the spectra of the X^{3-} exciton where a singlet-triplet transition is expected (and should be observable) as function of the dot height. Beyond the understanding of the physics, the quantitative results given here can serve as guide for experimentalists when analyzing charged exciton spectra, especially for the positively charged dots where only little has been reported until now. Conversely, our results might be useful for crystal growers who want to achieve certain optical property by tuning the dot size and composition.

This work was supported by the U.S. Department of Energy, SC-BES-DMS Grant No. DEAC36-98-GO10337.

[1] H. Drexler *et al.*, Phys. Rev. Lett. **73**, 2252 (1994).
[2] R.C. Ashoori *et al.*, Phys. Rev. Lett. **68**, 3088 (1992).
[3] S. Cortez *et al.*, Phys. Rev. Lett. **89**, 207401 (2002).
[4] I.A. Akimov *et al.*, Appl. Phys. Lett. **81**, 4730 (2002).
[5] L. Landin *et al.*, Science **280**, 262 (1998).
[6] D.V. Regelman *et al.*, Phys. Rev. B **64**, 165301 (2001).
[7] A. Hartmann *et al.*, Phys. Rev. Lett. **84**, 5648 (2000).
[8] J.J. Finley *et al.*, Phys. Rev. B **63**, 161305 (2001).
[9] F. Findeis *et al.*, Appl. Phys. Lett. **78**, 2958 (2001).
[10] F. Findeis *et al.*, Phys. Rev. B **63**, 121309 (2001).
[11] M. Baier *et al.*, Phys. Rev. B **64**, 195326 (2001).
[12] K.F. Karlsson *et al.*, Acta. Phys. Pol. **100**, 387 (2001).
[13] A. Ashmore *et al.*, Physica E (Amsterdam) **13**, 127 (2002).
[14] A. Zrenner *et al.*, Physica E (Amsterdam) **13**, 95 (2002).
[15] D.V. Regelman *et al.*, Physica E (Amsterdam) **13**, 114 (2002).
[16] K. Karlsson *et al.*, Physica E (Amsterdam) **13**, 101 (2002).
[17] T. Walther *et al.*, Phys. Rev. Lett. **86**, 2381 (2001).
[18] R. Kegel *et al.*, Phys. Rev. B **63**, 035318 (2001).
[19] A. Zunger, Phys. Status Solidi A **190**, 467 (2002).
[20] R.J. Warburton *et al.*, Phys. Rev. B **58**, 16 221 (1998).
[21] U. Hohenester and E. Molinari, Phys. Status Solidi B **221**, 19 (2000).
[22] P. Lelong and G. Bastard, Solid State Commun. **98**, 819 (1996).
[23] L.-W. Wang and A. Zunger, Phys. Rev. B **59**, 15 806 (1999).
[24] A. Franceschetti *et al.*, Phys. Rev. B **60**, 1819 (1999).
[25] R. Resta, Phys. Rev. B **16**, 2717 (1977).
[26] G. Bester, S.V. Nair, and A. Zunger, Phys. Rev. B **67**, 161306 (2003).
[27] A.J. Williamson, L.-W. Wang, and A. Zunger, Phys. Rev. B **62**, 12 963 (2000).
[28] R.J. Warburton *et al.*, Nature (London) **405**, 926 (2000).
[29] R.J. Warburton *et al.* Physica E **9**, 124 (2001).
[30] Y. Ducommun *et al.* Phys. Status Solidi B **224**, 325 (2001).
[31] P.W. Fry *et al.* Phys. Rev. Lett. **84**, 733 (2000).